Journal of Solid State Chemistry **159,** 191–197 (2001)
doi:10.1006/jssc.2001.9150, available online at http://www.idealibrary.com on IDEAL®

A NiAs/Ni_2In-Type Phase $Ni_{1+x}Sn$ ($0.35 < x < 0.45$) with Incommensurate Occupational Ordering of Ni

A. Leineweber,[1] M. Ellner, and E. J. Mittemeijer

Max Planck Institute for Metals Research, Seestraße 92, 70174 Stuttgart, Germany

Received December 4, 2000; in revised form February 26, 2001; accepted March 15, 2001; published online May 11, 2001

The previously reported, ordered low-temperature NiAs/Ni_2In-type phase $Ni_{1+x}Sn$ comprises in the concentration range $0.35 < x < 0.53$ in fact two separate, ordered phases. Both phases are based on a NiAs-type arrangement, "NiSn," with the additional Ni atoms distributed over the trigonal–bipyramidal interstitial sites in an ordered way. Around the ideal composition Ni_3Sn_2 ($0.45 < x < 0.53$), the earlier reported commensurate structure occurs, termed the "LT phase," in which the long-range ordering leads to *Pbnm* symmetry with unit cell parameters $a_{LT} \approx 2a_{HT}$, $b_{LT} \approx 3^{1/2}a_{HT}$, $c_{LT} \approx c_{HT}$, where the subscript HT refers to the corresponding, disordered hexagonal high-temperature phase. For lower Ni contents ($0.35 < x < 0.45$) an incommensurate phase, that is termed "LT' phase," occurs with a crystal structure closely related to the LT phase. According to X-ray powder diffraction and selected area electron diffraction analyses, the average unit cell exhibits orthorhombic *Cmcm* symmetry, has unit cell parameters $a_{orth} \approx a_{HT}$, $b_{orth} \approx 3^{1/2}\, b_{HT}$, $c_{orth} \approx c_{HT}$, and a modulation vector $\vec{q} = \alpha\vec{a}^*_{orth}$ with $\alpha \approx 0.493$ for $x = 0.44$ and $\alpha \approx 0.428$ for $x = 0.35$. The LT phase may be regarded as a "lock-in" phase of the LT' phase with $\alpha = \frac{1}{2}$. A model for the long-range occupational ordering of Ni on the trigonal–bipyramidal interstitial sites has been suggested.

Key Words: **incommensurate structures; occupational ordering; X-ray powder diffraction.**

1. INTRODUCTION

The crystalline phases observed near the composition Ni_3Sn_2 in the system Ni–Sn (1) belong to the large group of NiAs/Ni_2In type phases (2, 3). The crystal structures of these phases are based on a NiAs type substructure "Ni(1)Sn" (*hcp* arrangement of Sn with Ni(1) on all octahedral sites) with the additional Ni(2) atoms occupying partially, in a more or less ordered way, the trigonal–bipyramidal interstitial sites in the Sn arrangement. If the trigonal–bipyramidal interstitial sites were completely filled, the composition "Ni_2Sn" with Ni_2In-type structure (4) would result. However, the Ni_3Sn_2 ($= Ni(1)_1Ni(2)_xSn$) phase field covers a composition range of only about $0.35 < x < 0.65$ (1).

The observed c/a axial ratios of the different phases in the Ni_3Sn_2 phase field are much smaller ($c/a \approx 1.26$) than the value of an ideal *hcp* arrangement ($c/a \approx 1.633$). Nevertheless, it is very useful to discuss the crystal structure emanating from the *hcp*-type arrangement of the Sn atoms and also from the *hcp*-type arrangement of the trigonal–bipyramidal interstitial sites themselves. Considering ordering of Ni(2) on the latter sites only, the possible structure types straightforwardly follow from the types of substitutional ordering that can be constructed for alloys with a *hcp*-type structure (5).

At relatively high temperatures ($T > \approx 790$ K, dependent on composition) a phase, here called HT phase, without long-range order of Ni(2) and exhibiting $P6_3/mmc$ symmetry (unit cell parameters a_{HT}, c_{HT}, number of formula units $Z(Ni_{1+x}Sn) = 2$; Sn on $2c$ Wyckoff-site: $\frac{1}{3}, \frac{2}{3}, \frac{1}{4}$; Ni(1) on $2a$: 0,0,0; Ni(2) on $2d$: $\frac{1}{3}, \frac{2}{3}, \frac{3}{4}$ with an occupancy of x), is stable (6, 7). The HT phase can be retained easily by quenching. Electron diffraction revealed diffuse scattering ascribed to short-range occupational ordering of the Ni(2) atoms in association with corresponding atomic displacements (8).

At relatively low temperatures, long-range ordering of the Ni(2) atoms occurs as revealed by the splitting of fundamental reflections and the occurrence of superstructure reflections (6, 9, 10). For $x = 1/2$ (i.e., Ni_3Sn_2) an ideal crystal structure of this phase, here called the LT phase, was determined by X-ray single-crystal diffraction (10); it has unit cell parameters $a_{LT} \approx 2a_{HT}$, $b_{LT} \approx 3^{1/2}\, a_{HT}$, $c_{LT} \approx c_{HT}$ and shows *Pbnm* symmetry ($Z(Ni_{1+x}Sn) = 8$, in the original work the *Pnam* setting was chosen; the standard setting is *Pnma* (11). The occupational ordering scheme for the Ni(2) atoms in the LT phase is depicted in Fig. 1. According to Ref. (6) the LT phase occurs for $0.35 < x < 0.55$. For higher Ni contents long-range ordering of Ni(2) would not occur (6).

In this paper, an until now unknown incommensurate LT′ phase $Ni_{1+x}Sn$ is reported that is closely related to the

[1] To whom correspondence should be addressed. E-mail: leineweber@mf.mpi-stuttgart.mpg.de.

0022-4596/01 $35.00

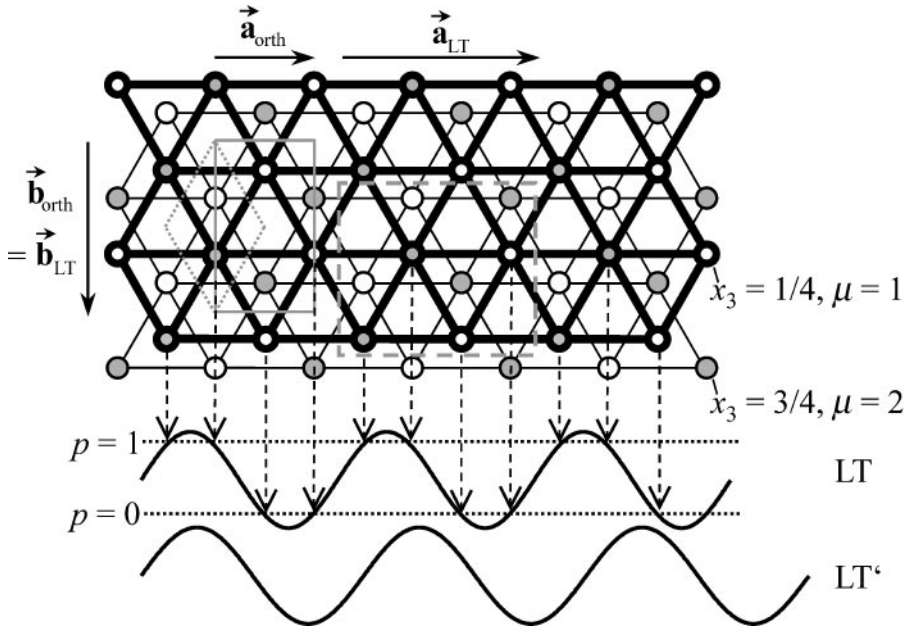

FIG. 1. Schematic illustration of the Ni(2) atom distribution in the ideal LT Ni_3Sn_2 structure (projected view along the $\vec{c}_{orth}$ direction). For clarity, only the *hcp*-type substructure formed by the trigonal–bipyramidal interstitial sites (*hcp* unit cell of the HT phase is indicated with grey dotted lines) is shown. Sites occupied by Ni(2) have been indicated gray, unoccupied sites are shown in white. The displacements of the Ni(2) sites from their ideal positions and the orthorhombic distortion of the lattice have not been indicated. The box drawn with full gray lines shows the unit cell of the *C*-centered orthorhombic average structure, the box drawn with dashed gray lines shows the unit cell of the LT phase (*Pbnm* symmetry; taking into account the different choices of origin between the *C*-centered orthorhombic and the LT unit cells). In the bottom part of the figure, the occupational modulation wave $p(\mu, \vec{\mathbf{T}})$ for the ideal LT Ni_3Sn_2 case at $x = \frac{1}{2}$ (see Section 3.3) has been depicted giving the occupancies of the $\mu = 1$ Ni(2) positions as a function of $\vec{\mathbf{T}}$. p varies with the modulation vector $\vec{\mathbf{q}} = \frac{1}{2}\vec{\mathbf{a}}^*_{orth}$ along the direction $\vec{\mathbf{a}}_{orth}$. The dashed arrows indicate the values $p(1, \vec{\mathbf{T}})$ at the positions of the corresponding trigonal–bipyramidal interstitial sites, giving either 0 and 1 as occupancies for the Ni(2). For the LT′ case the wave becomes incommensurate and it is only schematically shown below the wave for the LT phase.

LT phase. The new phase occurs in the compositional range $0.35 < x < 0.45$, where the LT phase does not occur in marked contrast with Ref. (6); i.e. the LT phase is found here only in the range $0.45 < x < 0.53$.

2. EXPERIMENTAL

2.1. Preparation, Chemical Analysis, and Heat Treatment

$Ni_{1+x}Sn$ alloys (for compositions, see Table 1) were prepared from Ni sheets (1 mm thickness, 99.98 mass%, Goodfellow) and Sn bars (99.999 mass%, Heraeus). The starting materials (total mass 32–35 g) were melted by induction heating and cast into water-cooled cylindrical moulds to give rods of a diameter of 8 mm and a length of 50 mm. The top and bottom parts of the cast rods were removed. The remaining material was sealed in quartz tubes and subjected to an homogenization treatment for 3 days at 473 K (The treatment at 473 K was chosen in order to remove Sn rich inhomogeneities of the cast material before their melting.) The material was subsequently treated for 3 days at 1023 K followed by water quenching. Thereby, homogeneous specimens of the high-temperature phase were obtained.

In order to produce samples with the ordered low-temperature phase, pieces of the above-mentioned samples of the homogenized HT phase were resealed in quartz tubes and heated for 5 days at 673 K followed by water quenching.

Chemical analysis performed by X-ray fluorescence analysis (accuracy ± 0.3 mass% for Ni, ± 0.4 mass% for Sn) showed that within experimental accuracy the sample compositions are equal to the values calculated from the amounts of the starting materials used for the melting. The oxygen contents are negligibly small: only 0.002(1)–0.003(1) mass% (carrier gas hot extraction).

2.2. X-Ray Powder Diffraction and TEM

X-ray diffraction data were collected on a Phillips X′Pert Plus diffractometer equipped with a primary monochromator selecting Cu$K\alpha 1$ radiation. The diffractometer samples were thin layers of the powdered alloys with or without internal Ge standard powder measured at 298(1) K. The 2θ diffraction-angle range covered $10^\circ < 2\theta < 120^\circ$.

For unit cell parameter determination, the positions of the fundamental reflections of $Ni_{1+x}Sn$ and of the

TABLE 1
Unit Cell Parameters and Modulation Vector Determined for the LT or LT′ Phase Resulting from HT Phase Samples by Heat Treatment for 5 Days at 673 K Followed by Water Quenching

x with respect to $Ni_{1+x}Sn$	a_{orth} (Å)	b_{orth} (Å)	c_{orth} (Å)	α according to $\vec{q} = \alpha\vec{a}^*_{orth}$
0.532 (LT)	4.0875(4)	7.1340(6)	5.1973(7)	$\frac{1}{2}$
0.500 (LT)	4.0742(3)	7.1223(4)	5.1937(5)	$\frac{1}{2}$
0.469 (LT)	4.0678(3)	7.1090(4)	5.1856(5)	$\frac{1}{2}$
0.439 (LT′)	4.0648(2)	7.0966(3)	5.1759(3)	0.49329(10)
0.410 (LT′)	4.0595(2)	7.0824(3)	5.1646(3)	0.45171(7)
0.380 (LT′)	4.0531(1)	7.0702(2)	5.1578(2)	0.43394(7)
0.352 (LT′)	4.0528(3)	7.0561(5)	5.1489(7)	0.42802(16)

reflections of Ge were determined in the range $26° < 2\theta < 68°$ using the programme ProFit (12). The 2θ scale was calibrated using the Ge standard reflections ($a_{Ge} = 5.6574$ Å (13)). The resulting positions of the $Ni_{1+x}Sn$ reflections were used as input for a least-squares fitting procedure (ASIN (14)) yielding the cell parameters.

The magnitude of the modulation vector of the incommensurate structure (LT′ phase) was determined using the Full Powder Pattern fitting Programme SIMPRO (15) in the angular range of $26° < 2\theta < 55°$.

Selected area electron diffraction was performed using a Transmission Electron Microscope (TEM) JEM 2000FX. Samples for TEM consisted of powdered $Ni_{1.41}Sn$ (annealed for 5 days at 673 K and water quenched) dispersed in ethanol and then brought onto a holey-carbon-coated copper grid.

3. RESULTS AND DISCUSSION

3.1. Occurrence of the HT and LT Phases

X-ray powder diffraction data recorded from the specimens prepared from the homogenized rods (3 days at 473 K, 3 days at 1023 K, water quenching) indicate that the specimens consist of the disordered, hexagonal HT phase, as expected (6). After the specimens were annealed for 5 days at 673 K followed by water quenching, the X-ray powder diffraction patterns were recorded for all alloys indicated in Table 1 and show splitting of all fundamental reflections except those with the indices $00l_{HT}$ and, moreover, additional reflections indicate superstructure formation.

The occurrence of splitting of the fundamental reflections can be described in terms of a new *C*-centered orthorhombic unit cell with the unit cell parameters $a_{orth} \approx a_{HT}$, $b_{orth} \approx 3^{1/2}a_{HT}$, $c_{orth} \approx c_{HT}$ ($Z(Ni_{1+x}Sn) = 4$). The orthorhombic distortion may be quantified by the ratio $(a_{orth})/(b_{orth}/3^{1/2})$, which is always smaller than one, as in Ref. (6). (This contrasts with unit cell parameters extracted from Weissenberg photographs in Ref. (10), which suggest $(a_{orth})/(b_{orth}/3^{1/2}) > 1$. However, the standard deviations given in Ref. (10) make clear that the accuracy was too low to determine even the "direction" of the distortion of the unit cell unambiguously.)

For the samples with $x = 0.53$, 0.50, and 0.47 (cf. Table 1) the observed superstructure reflections correspond with the previously reported LT phase superstructure (6, 10), implying a doubling of the a_{orth} unit cell parameter and thus $a_{LT} = 2\,a_{orth} \approx 2\,a_{HT}$, $b_{LT} \approx 3^{1/2}a_{HT}$, $c_{LT} \approx c_{HT}$ ($Z(Ni_{1+x}Sn) = 8$) for the LT unit cell exhibiting *Pbnm* symmetry (cf. Figs. 1 and 2a).

3.2. Occurrence of the Incommensurate LT′ Phase

In marked contrast with Ref. (6), for lower Ni contents ($x = 0.44$, 0.41, 0.38, 0.35) the superstructure reflections cannot simply be assigned to the presence of a LT-type structure. (Heat treatment procedures other than the described 5 days at 673 K followed by water quenching were performed for $0.35 < x < 0.45$, also as described in Ref. (6). Neither of these procedures led to the appearance of the LT phase.) With respect to the positions of the fundamental reflections, the superstructure reflections are shifted to higher or lower 2θ values as compared to those expected for the LT phase superstructure. For $x = 0.44$ these shifts are very small, but they increase considerably for decreasing values of x.

The indicated features of the diffraction data for $x \leq 0.44$ can be explained by the presence of an incommensurate superstructure phase, which is called here LT′ phase. All superstructure reflections observed in the X-ray diffraction patterns of the LT′ phase samples can be regarded as first-order satellite reflections with respect to the reciprocal lattice corresponding to the the basis vectors of the abovementioned *C*-centered orthorhombic unit cell as derived directly from the fundamental reflections ($a_{orth} \approx a_{HT}$, $b_{orth} \approx 3^{1/2}a_{HT}$, $c_{orth} \approx c_{HT}$; see above). The positions of these satellites in reciprocal space are described by $\vec{G}_{orth} + m_{LT'}\cdot\vec{q}$, where $\vec{G}_{orth}$ describes the positions of the fundamental reflections, and where $m_{LT'} = \pm 1$ and $\vec{q}$ denotes the modulation vector according to $\vec{q} = \alpha\vec{a}^*_{orth}$ ($\vec{a}^*_{orth}$ is the reciprocal lattice vector of $\vec{a}_{orth}$). This interpretation was confirmed by selected area electron diffraction of a sample $Ni_{1.41}Sn$. The electron diffraction pattern, given in Fig. 3, shows besides first-order satellites additionally the presence of some second-order satellites, matching the above principle with $m_{LT'} = \pm 2$ (for electron diffraction patterns of the commensurate LT phase Ni_3Sn_2, see Fig. 2d of Ref. (8)).

The length of the modulation vector $\vec{q} = \alpha\vec{a}^*_{orth}$ was determined for the different sample compositions by full-pattern fits to the X-ray powder diffraction data (e.g., Fig. 2). The values of α vary from 0.428 for $x = 0.35$ to 0.493 for $x = 0.44$ (see Table 1). A plot of $(\frac{1}{2} - \alpha)$ as a function of x is given in

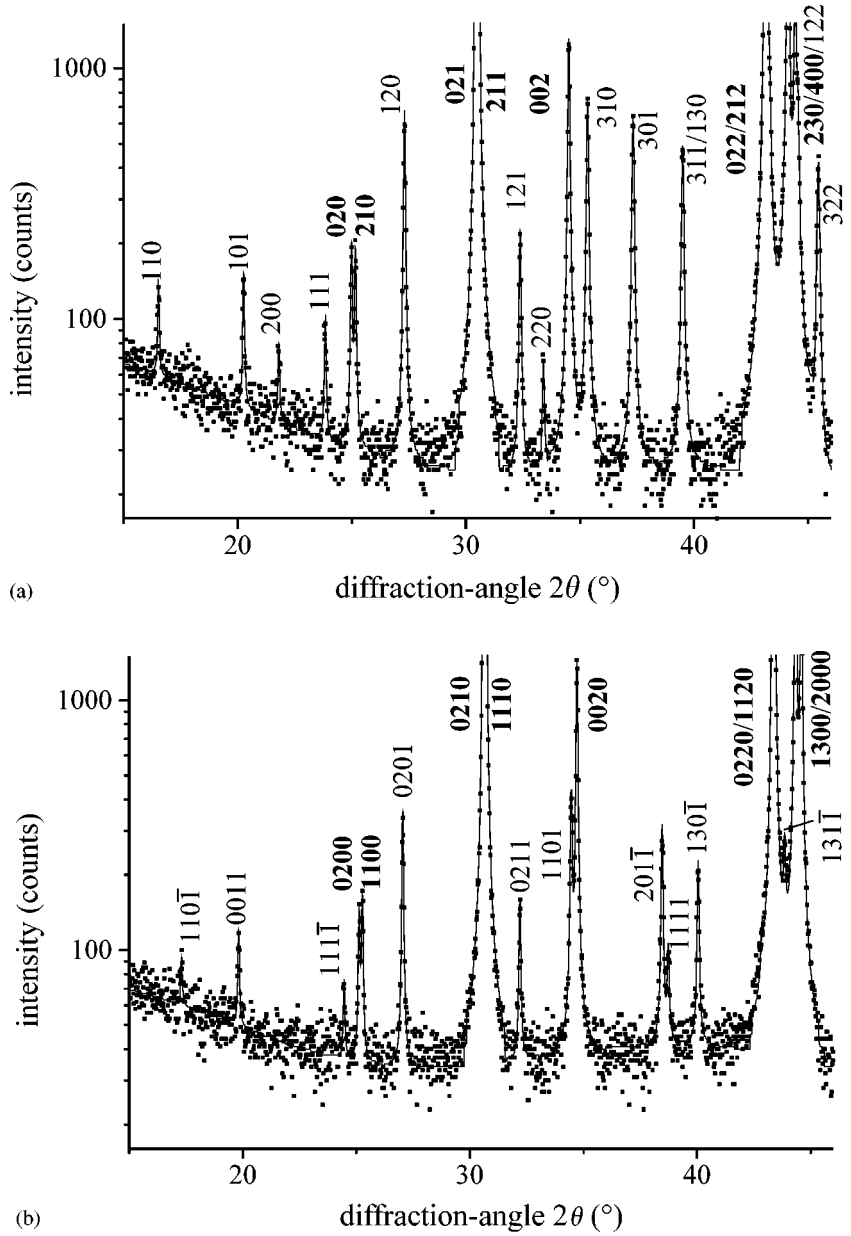

FIG. 2. Powder diffraction patterns of the LT phase $Ni_{1.50}Sn$ (a) and the LT′ phase $Ni_{1.41}Sn$ (b); logarithmic intensity scale. Reflections are labelled hkl_{LT} and $hklm_{LT'}$, respectively. The strongest reflections have been truncated with respect to their intensity. The maximum intensities recorded are 5200 counts for 021/211 ($Ni_{1.50}Sn$) and 6200 counts for 0210/1110 ($Ni_{1.41}Sn$). Fundamental reflections hkl_{LT} and $hkl0_{LT'}$ have been labeled in the figure with bold; the other indicated reflections are superstructure/satellite reflections. For $Ni_{1.41}Sn$ only first-order satellites reflections, $hkl \pm 1_{LT'}$ have been observed, which are related to superstructure reflections of LT type $Ni_{1.50}Sn$ by $110\bar{1}_{LT'} \rightarrow 110_{LT}$, $0011_{LT'} \rightarrow 101_{LT}$, $111\bar{1}_{LT'} \rightarrow 111_{LT}$, $0201_{LT'} \rightarrow 120_{LT}$, $0211_{LT'} \rightarrow 121_{LT}$, $1011_{LT'} \rightarrow 310_{LT}$, $201\bar{1}_{LT'} \rightarrow 301_{LT}$, $1111_{LT'} \rightarrow 311_{LT}$, $130\bar{1}_{LT'} \rightarrow 130_{LT}$, $131\bar{1}_{LT'} \rightarrow 131_{LT}$ (131_{LT} is rather invisible because of overlap with strong fundamental reflections).

Fig. 4. Proceeding from low x toward $x \approx 0.45$, $(\frac{1}{2} - \alpha)$ falls to zero, i.e., $\alpha = \frac{1}{2}$. Thus, the structure of the LT phase can be described as commensurately modulated with $\alpha = \frac{1}{2}$, as confirmed by full pattern fits. The reflections of the LT′ phase, $hklm_{LT'}$, are related those of the LT phase, hkl_{LT}, by $2h_{LT'} + m_{LT'} = h_{LT}$, $k_{LT'} = k_{LT}$ and $l_{LT'} = l_{LT}$. Most of the superstructure reflections of the LT phase (those with uneven h_{LT}) can be conceived as first-order satellites; a few weak superstructure reflections with even h_{LT} are second-order satellites, which are not observed for the LT′ phase in the X-ray diffraction patterns (Fig. 2), but are observed in the electron diffraction patterns (Fig. 3).

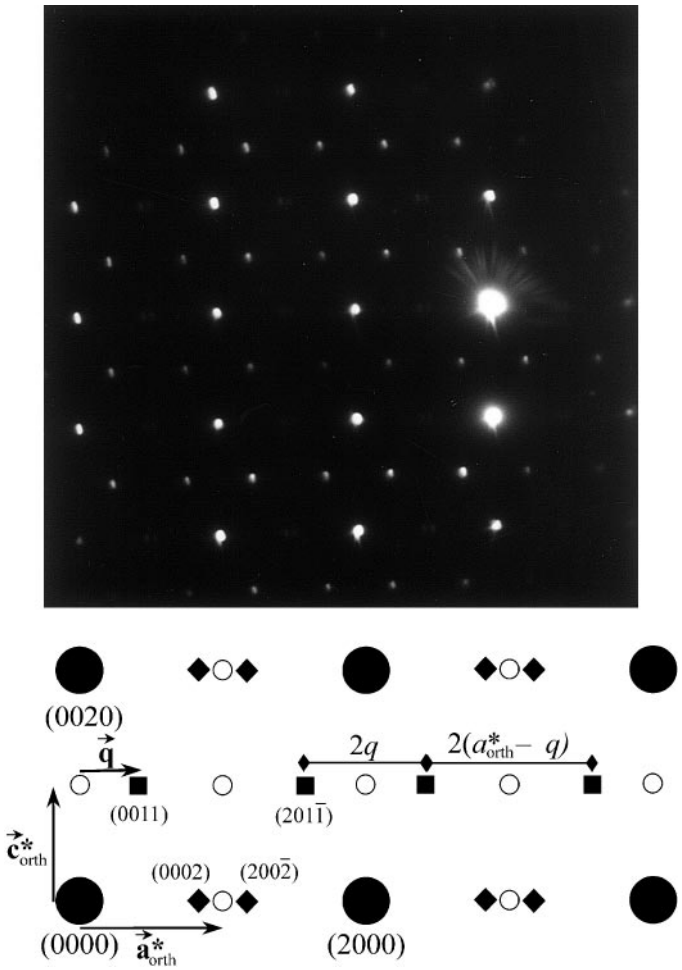

FIG. 3. Results of selected area electron diffraction performed on LT′ $Ni_{1.41}Sn$ powder: $[010]_{orth}$ zone pattern (top) showing reflections $h0lm_{LT'}$. Interpretation is provided on the bottom: (●) observed fundamental reflections; (○) extinct fundamental reflections; (■) observed first-order satellites ($m_{LT'} = \pm 1$), (◆) observed second-order satellites ($m_{LT'} = \pm 2$). The splitting of the second-order satellites (e.g., (2002) and (0002)) as well as the nonequal distances $2q$ and $2(a^*_{orth} - q)$ between the first-order satellites illustrate the incommensurability of the LT′ structure. For the commensurate LT structure the second-order satellites degenerate to one single reflection and the discussed distances between the first-order satellites become equal (Fig. 2d of Ref. (8)) leading to $\vec{a}^*_{LT} = \vec{a}^*_{orth}/2$.

3.3. *Model for the Ordered Ni(2) Atom Distribution in the LT′ Phase*

A simple model for the distribution of the Ni(2) atoms on the *hcp*-type substructure formed by the trigonal–bipyramidal interstitial sites in the incommensurate LT′ phase may be derived from the known structure for the commensurate LT phase, using the concentration wave/occupational modulation wave description of the occupancies (16, 17). Some main principles for such concentration waves for the *hcp* type case were already derived in Ref. (18), focusing especially on superstructures deriving from selected modulation vectors, $\vec{q}$, corresponding to the high-symmetry points in the first Brillouin-zone of the hexagonal lattice. The modulation vectors $\vec{q}$ for the superstructures pertaining to the LT and LT′ phase, expressed relative to the unit cell of the hexagonal HT phase, are $\vec{q} = \frac{1}{4}(\vec{a}^*_{HT} + \vec{b}^*_{HT})$ and $\vec{q} = \alpha/2(\vec{a}^*_{HT} + \vec{b}^*_{HT})$, respectively. (This takes into account the relation between the reciprocal lattices of the *C*-centered orthorhombic unit cell and the unit cell of the HT phase: $\frac{1}{2}(\vec{a}^*_{HT} + \vec{b}^*_{HT}) = \vec{a}^*_{orth}$ and $\frac{1}{2}(-\vec{a}^*_{HT} + \vec{b}^*_{HT}) = \vec{b}^*_{orth}$.) These do not belong to the selection of vectors discussed in Ref. (18).

Here, the concentration wave description for the LT phase will be derived, however, starting with the *C*-centered orthorhombic unit cell a_{orth}, b_{orth}, c_{orth} giving $\vec{q} = \frac{1}{2}\vec{a}^*_{orth}$. Then, the concentration wave description for the LT′ phase with $\vec{q} = \alpha\vec{a}^*_{orth}$ follows straightforwardly.

The orthorhombic unit cell results from a simple distortion of the unit cell of the HT phase, with $P6_3/mmc$ symmetry, leading to *Cmcm* and the atomic positions Sn 4*c*: 0, $\approx 0.33, \frac{1}{4}$; Ni(1) 4*a*: 0,0,0; Ni(2) 4*c*: 0, $\approx 0.67, \frac{1}{4}$, occupancy *x*. All types of sites are of fourfold multiplicity, however, two of the four positions of each type of site can be generated by lattice translation $\vec{T} = 1/2(\vec{a}_{orth} + \vec{b}_{orth})$. This orthorhombic structure serves as the average structure (17) for the LT and LT′ phases. Starting from this average structure the modulated structures are obtained by spatially modulating the occupancy of the Ni(2) site with the wave vector $\vec{q}$.

In order to set up the concentration wave, only the two Ni(2) positions, which are inequivalent by translation, must be considered: 0, $\approx 0.67, \frac{1}{4}$ and 0, $\approx 0.33, \frac{3}{4}$. These two Ni(2) positions will now be labeled as $\mu = 1, 2$. Assuming a simple sine-like modulation for the occupancies *p*, *p* can be writted

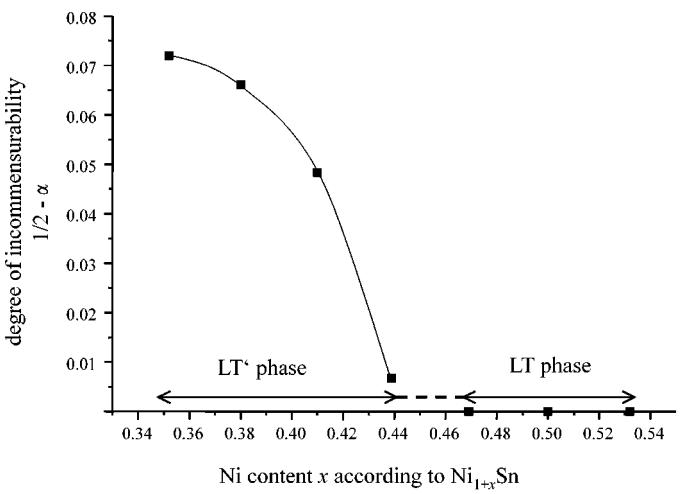

FIG. 4. $Ni_{1+x}Sn$: "Degree of incommensurability," $1/2 - \alpha$ with α according to $\vec{q} = \alpha\vec{a}^*_{orth}$ as a function of Ni content, *x*. The detailed character of the transition LT↔LT' at $x = 0.45$ cannot be deduced from the present data.

as function of the lattice translation vector, $\vec{\mathbf{T}} = u\vec{\mathbf{a}}_{\text{orth}} + v\vec{\mathbf{b}}_{\text{orth}} + w\vec{\mathbf{c}}_{\text{orth}}$ or $(u + \frac{1}{2})\vec{\mathbf{a}}_{\text{orth}} + (v + \frac{1}{2})\vec{\mathbf{b}}_{\text{orth}} + w\vec{\mathbf{c}}_{\text{orth}}$ with u, v, w as integers, according to

$$p(\mu, \vec{\mathbf{T}}) = x + \eta \cdot \gamma(\mu) \sin(2\pi\vec{\mathbf{q}} \cdot \vec{\mathbf{T}} + \varphi)$$

with $\vec{\mathbf{q}} = 1/2\vec{\mathbf{a}}^*_{\text{orth}}$ for the LT phase and $\vec{\mathbf{q}} = \alpha\vec{\mathbf{a}}^*_{\text{orth}}$ for the LT′ phase. The order parameter η determines the amplitude of the occupational modulation. The coefficients $\gamma(1)$ and $\gamma(2)$ determine the symmetry of the resulting ordered structure. There are two high symmetric possibilities: $\gamma(1) = \gamma(2)$ and $\gamma(1) = -\gamma(2)$ (18). The first possibility $\gamma(1) = \gamma(2)$ means that the Ni(2) positions 0, ≈ 0.67, $\frac{1}{4}$ and 0, ≈ 0.33, $\frac{3}{4}$, corresponding to a certain value of $\vec{\mathbf{T}}$, are both filled up or depleted at the same time, whereas $\gamma(1) = -\gamma(2)$ means that one site is filled and the other one is depleted.

For the ideal LT Ni_3Sn_2 structure (with $x = \frac{1}{2}$) $\gamma(1) = -\gamma(2)$ obviously holds (Fig. 1). The modulation occurs with the wave vector $\vec{\mathbf{q}} = \frac{1}{2}\vec{\mathbf{a}}^*_{\text{orth}}$ (parallel to $\vec{\mathbf{a}}$), and, for the structure as shown in Fig. 1, the phase (see above formula) is $\varphi = 3/4\pi$ (structures with $\varphi = \frac{1}{4}\pi + n\pi/2$ are equivalent). Taking $\gamma(1) = 1$ and $\gamma(2) = -1$ and the order parameter $\eta = 2^{-1/2}$ gives occupancies $p(\mu, \vec{\mathbf{T}})$ of either 1 or 0 at the positions of Ni(2) (cf. above formula and note that x is the average occupancy).

All observed first-order satellite reflections of the incommensurate LT′ phase, $hklm_{\text{LT}'}$ with $m_{\text{LT}'} = \pm 1$, have their analogues in the LT phase superstructure reflections, hkl_{LT} with uneven h_{LT} (cf. Figs. 2a and 2b). Therefore, $\gamma(1) = -\gamma(2)$, which holds for the LT phase, must be preserved in the LT′ phase. The modulation wave vector then changes to $\vec{\mathbf{q}} = \alpha\vec{\mathbf{a}}^*_{\text{orth}}$, instead of being equal to $\frac{1}{2}\vec{\mathbf{a}}^*_{\text{orth}}$ as for the LT phase; all values of φ now give the same distribution of Ni(2), as a change of φ means only a change in origin. Addition of higher harmonic terms in the above formula for $p(\mu, \vec{\mathbf{T}})$ requires assigning appropriate values to the original and additional η parameters such that the occupancies are within the range $0 \le p(\mu, \vec{\mathbf{T}}) \le 1$.

The similarities between the LT and LT′ phases become also apparent from the reflection conditions. Those of the LT phase with *Pbnm* symmetry are preserved in the LT′ phase according to the X-ray and electron diffraction patterns. For the LT phase the reflection conditions are $0kl_{\text{LT}}$ with $k_{\text{LT}} = 2n$ and $h0l_{\text{LT}}$ with $h_{\text{LT}} + l_{\text{LT}} = 2n$. As mentioned above, the indices $hklm_{\text{LT}'}$ are related to hkl_{LT} by $2h_{\text{LT}'} + m_{\text{LT}'} = h_{\text{LT}}$ as well as $k_{\text{LT}'} = k_{\text{LT}}$ and $l_{\text{LT}'} = l_{\text{LT}}$. The reflection conditions become then for the LT′ phase $hkl2\ \bar{h}_{\text{LT}'}$ with $k_{\text{LT}'} = 2n$ and $h0lm_{\text{LT}'}$ with $2h_{\text{LT}'} + m_{\text{LT}'} + l_{\text{LT}'} = 2n$, which is equivalent to $m_{\text{LT}'} + l_{\text{LT}'} = 2n'$. The last reflection condition for the LT′ suggests that the glide plane *.c.*, which transforms the two trigonal–bipyramidal sites $\mu = 1, 2$ corresponding to one value of $\vec{\mathbf{T}}$ into each other, is associated with a phase shift of π for the modulation wave, which results in the condition $\gamma(1) = -\gamma(2)$. This can be expressed by the four-dimensional symmetry operation x_1, $-x_2$, $x_3 + \frac{1}{2}$, $x_4 + \frac{1}{2}$ (x_1, x_2, x_3 are the fractional coordinates in the three-dimensional space and one can take here $x_4 = \vec{\mathbf{q}} \cdot \vec{\mathbf{T}}$, (19)). Finally, the reflection conditions observed for the LT' phase lead to the (3 + 1)-dimensional superspace group $Cmcm(\alpha 00)0s0$ (19). (For $Cmcm(\alpha 00)0s0$ the reflection condition $hkl2\ \bar{h}_{\text{LT}'}$ with $k_{\text{LT}'} = 2n$ is only strictly required for $2h_{\text{LT}'} = -m_{\text{LT}'} = 0$. For $2h_{\text{LT}'} = -m_{\text{LT}'} = 2, 4, 6\ldots$ also reflections with $k_{\text{LT}'} \neq 2n$ may occur, being second-, fourth-, sixth-order satellites. These were, however, not observed.) Indeed, preliminary results of Rietveld refinements of powder diffraction data of the LT′ phase using JANA2000 (20) confirm the model for the distribution of Ni(2) presented here (21).

The observation that for Ni(2) contents smaller than about $x = 0.45$ the value of α becomes smaller than $\frac{1}{2}$, i.e., the structure becomes incommensurate, may be associated with the appearance of a specific diffuse scattering in the HT phase (8): the positions of the most prominent maxima of this diffuse intensity in the reciprocal space "move" (in this case largely proportional) with composition into the same direction as the first-order satellites do for the LT′ phase (cf. Fig. 4).

With respect to the occurrence of the commensurate LT and incommensurate LT′ $Ni_{1+x}Sn$ phases in the Ni–Sn system, a similar situation has been reported for the system Mn–Sn (22, 23). A commensurate phase Mn_3Sn_2 isotypic to LT Ni_3Sn_2 exists. At higher Mn contents (separated by a rather extended two-phase field from Mn_3Sn_2) incommensurate phases were observed (22, 23), one being Mn_8Sn_5 ($Mn_{1.6}Sn$). The structure of Mn_8Sn_5 was determined and refined using X-ray single crystal diffraction (23) and selected area electron diffraction (22, 23). The super-space group symmetry was, as here for the LT′ phase, $Cmcm(\alpha 00)0s0$ with an average structure with unit cell parameters a_{orth}, b_{orth}, c_{orth}, and a modulation vector $\vec{\mathbf{q}} = \alpha\vec{\mathbf{a}}^*_{\text{orth}}$ with $\alpha = 0.616$. The main difference with the present LT′ phase is that the α value for $Mn_{1.6}Sn$ is larger than $\frac{1}{2}$ ($\alpha = \frac{1}{2}$, denontes the commensurate case). Here, for LT′ $Ni_{1+x}Sn$ with compositions of $x < 0.5$ one finds $\alpha < \frac{1}{2}$. Detailed comparison of the LT′ $Ni_{1+x}Sn$ and Mn_8Sn_5 phases is only possible after structure refinement of the incommensurate phase structures in $Ni_{1+x}Sn$ has been performed (21).

ACKNOWLEDGMENTS

The assistance of Mr. P. Kopold and Dr. W. Sigle with the electron diffraction measurements is gratefully acknowledged.

REFERENCES

1. P. Nash and A. Nash, *Bull. Alloy Phase Diagrams* **6,** 350 (1985).
2. S. Lidin, *Acta Crystallogr. Sect. B: Struct. Sci.* **54,** 97 (1998).

3. S. Lidin and A.-K. Larsson, *J. Solid State Chem.* **118,** 313 (1995).
4. F. Laves and H. J. Wallbaum, *Z. Angew. Mineralog.* **4,** 17 (1941).
5. J. Hauck and K. Mika, *Z. Kristallogr.* **214,** 443 (1999).
6. H. Fjellvåg and A. Kjekshus, *Acta Chem. Scand. A* **40,** 23 (1986).
7. M. Ellner, *J. Less-Common. Met.* **48,** 21 (1976).
8. A.-K. Larsson, R. L. Withers, and L. Stenberg, *J. Solid State Chem.* **127,** 222 (1996).
9. O. Nial, *Svensk. Kem. Tidskr.* **59,** 172 (1947).
10. P. Brand, *Z. Anorg. Allg. Chem.* **353,** 270 (1967).
11. Th. Hahn (Ed.), "International Tables for Crystallography," Vol. A, Space Group Symmetry. Kluwer Academic, Dordrecht, 1995.
12. E. J. Sonneveld and R. Delhez, "ProFit," Version 1.0c. Phillips Electronics N. V., 1996.
13. H. W. King, *Bull. Alloy Phase Diagrams* **2,** 402 (1981).
14. W. Jeitschko, E. Parthé, and K. Yvon, *J. Appl. Crystallogr.* **10,** 73 (1977).
15. H. Ritter and J. Ihringer, "SIMPRO Full Powder Pattern Fitting Programme," Version 1.2. University of Tübingen.
16. A. G. Khachaturyan, *Acta Metallurg.* **23,** 1089 (1975).
17. J. M. Perez-Mato, G. Madariaga, F. J. Zuñiga, and A. Garcia Arribas, *Acta Crystallogr. Sect. A: Found Crystallogr.* **43,** 216 (1987).
18. M. F. Zhorovkov, D. L. Fuks, and V. E. Panin, *Phys. Stat. Sol. B* **68,** 379 (1975).
19. A. J. C. Wilson, "International Tables for Crystallography," Vol. C, p. 391. Kluwer Academic, Dordrecht, 1992.
20. M. Dušek, V. Petříček, M. Wunschel, R. E. Dinnebier, and S. van Smaalen, *J. Appl. Crystallogr.*, accepted for publication.
21. A. Leineweber, M. Ellner, and E. J. Mittemeijer, unpublished.
22. M. Elding-Pontén, L. Stenberg, A.-K. Larsson, S. Lidin, and K. Ståhl, *J. Solid State Chem.* **129,** 231 (1997).
23. M. Elding-Pontén, L. Stenberg, S. Lidin, G. Madariaga, and J.-M. Pérez Mato, *Acta Crystallogr. Sect. B: Struct. Sci.* **53,** 364 (1997).